IEEE Photonics Journal
An IEEE Photonics Society Publication

Open Access

Broadband Photonic Microwave Signal Processor With Frequency Up/Down Conversion and Phase Shifting Capability

Volume 10, Number 1, February 2018

Tao Li
Erwin Hoi Wing Chan
Xudong Wang
Xinhuan Feng
Bai-Ou Guan
Jianping Yao

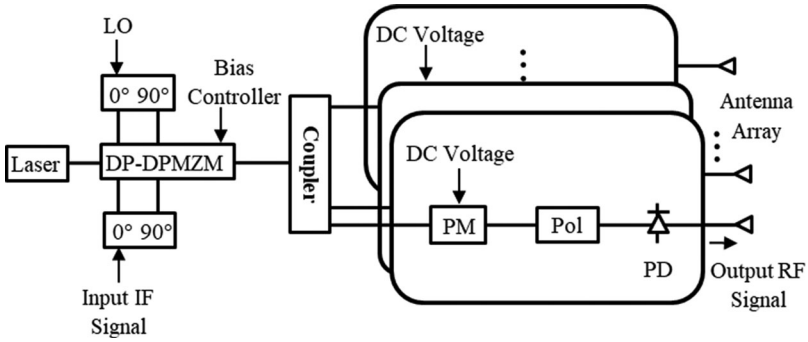

DOI: 10.1109/JPHOT.2017.2778287
1943-0655 © 2017 IEEE

IEEE photonics SOCIETY

IEEE

Broadband Photonic Microwave Signal Processor With Frequency Up/Down Conversion and Phase Shifting Capability

Tao Li,[1] Erwin Hoi Wing Chan ,[2] Xudong Wang ,[1] Xinhuan Feng ,[1] Bai-Ou Guan,[1] and Jianping Yao [3]

[1]Guangdong Provincial Key Laboratory of Optical Fiber Sensing and Communications, Institute of Photonics Technology, Jinan University, Guangzhou 510632, China
[2]School of Engineering and Information Technology, Charles Darwin University, Darwin, NT 0909, Australia
[3]School of Electrical Engineering and Computer Science, University of Ottawa, Ottawa, ON K1N 6N5, Canada

DOI:10.1109/JPHOT.2017.2778287

Manuscript received October 17, 2017; revised November 20, 2017; accepted November 25, 2017. Date of publication November 29, 2017; date of current version December 21, 2017. This work was supported in part by the National Natural Science Foundation of China under Grants 61501205 and 61771221, and in part by the Guangdong Natural Science Foundation under Grants 2014A030310419, 2015A030313322, and S2013030013302. Corresponding author: Xudong Wang (e-mail: txudong.wang@email.jnu.edu.cn).

Abstract: A new dual-function photonic microwave signal processing structure that has the ability to realize both frequency up/down conversion and RF/IF phase shifting, is presented. In the proposed signal processor, a dual-polarization dual-parallel Mach Zehnder modulator (DP-DPMZM) is used to generate an orthogonally polarized single RF/IF signal and local oscillator (LO) modulation sideband without an optical carrier. The optical phase difference between the two sidebands can be controlled by controlling a DC voltage applied to a $LiNbO_3$ electro-optic phase modulator that is connected after the DP-DPMZM. Beating between the two sidebands at a photodetector generates an RF/IF signal with a phase equal to the optical phase difference between the IF/RF signal and LO sidebands. The dual-function photonic microwave signal processor has a wide bandwidth and does not require a precise control of the laser wavelength. Experimental results demonstrate that a flat >-3 dB down/up conversion efficiency is achieved for an RF signal from 3.5 to 26.5 GHz and for an IF signal from 0.5 to 3 GHz, and a full 360° continuous phase shift of the output IF/RF signal.

Index Terms: Analog optical signal processing, microwave, fiber optics communications, radio frequency photonics.

1. Introduction

Phased array antennas have applications in meteorology [1], wireless communications [2] and radar [3] due to the advantages of multi-target tracking, ultrafast scanning and accurate beamforming. A phased array beamforming system usually consists of a number of phase shifters [4], to introduce different phase shifts to the microwave signals sent to or received from the antenna elements to enable beam scanning. Conventional microwave phase shifters are implemented by using switches [5], which cannot realize continuously tunable phase shifts, or adjustable waveguides [6], which has a limited response time. A typical transceiver/receiver phased array system also has mixers

for frequency up/down conversion [7]. Conventional microwave mixers have the problems such as limited bandwidth, low channel isolation and susceptible to electromagnetic interference.

The problems existing in a conventional electrical phase shifter and mixer can be solved by using photonics solutions [8]. Various techniques to implement microwave photonic phase shifters [9]–[12] and mixers [13]–[18] have been reported. However, until now there are only few structures that can realize both frequency conversion and phase shifting [17], [18]. The signal processor presented in [17] relies on the use of an optical filter to select only one sideband while suppressing the optical carrier and the other sideband. This technique requires that the wavelength of the laser source is precisely controlled to ensure that the unwanted carrier and the sideband to be filtered out by the optical filter. In addition, the processor presented in [17] has a limited operating bandwidth. This is due to a practical optical filter has a limited edge roll-off factor and hence the remaining sideband close to the optical carrier is partially or fully suppressed. This limits the lower frequency of the input RF signal, which is the reason why frequency down conversion of an RF signal was demonstrated with a relatively large lower frequency of 12 GHz. This also prevents the signal processor from being used for frequency up conversion. This is because the input IF signal in a transmitter for up conversion has low frequencies [19] and hence when the IF signal modulation sidebands are close to the optical carrier, they will be suppressed by the optical filter. Although the microwave photonic mixer given in [18] can be used for both frequency up and down conversion, the input RF/IF signal and LO are presented in the mixer output port when the optical carrier beats with the sidebands at the photodetector. The low isolation between the input and output ports is a problem [20] especially when the mixer is operating in the up conversion mode because the high-power LO is close to the up-converted RF signal. Furthermore it requires adjusting the bias voltages of two Mach Zehnder modulators to realize the phase shifting operation, which alters the mixer nonlinearity performance. Moreover the mixer is limited to sub-octave operation and has low conversion efficiency.

In this paper, we present a new photonic microwave signal processor that can overcome the aforementioned problems to enable both wideband frequency up and down conversion to be performed in the same structure. The signal processor can also realize a continuous 0°–360° IF/RF signal phase shift using only a single DC voltage control. The proposed dual-function photonic microwave signal processor is analyzed and experimentally demonstrated. Frequency down conversion of an RF signal from 3.5–26.5 GHz into 0.5–3 GHz and up conversion of an IF signal from 0.5–3 GHz to 3.5–26.5 GHz are achieved. The conversion efficiency of the mixer is also measured in both cases, which are around -2 dB with <2 dB ripples over the entire operating bandwidth. A 0°–360° phase shift on the down-converted IF signal and up-converted RF signal with almost no change (<2 dB) in the signal amplitude are also demonstrated.

2. Operation Principle

Fig. 1 shows the schematic of the proposed dual-function photonic microwave signal processor. A continuous wave (CW) light generated by a laser source is sent to a DP-DPMZM. A DP-DPMZM consists of two DPMZMs connected in parallel with a 90° polarization rotator in one of the DPMZM outputs. The RF/IF signal for down/up conversion is applied to the bottom DPMZM and the LO is applied to the top DPMZM. The two DPMZMs are biased in the way to generate only one sideband with the optical carrier being suppressed. This is done by biasing the two sub MZMs inside a DPMZM at the minimum transmission point, and biasing the main MZM at the quadrature point to introduce 90° optical phase difference between the two sub MZM outputs [21]. DP-DPMZMs are commercially available [22]. A commercial DP-DPMZM bias controller [23] can be used to simplify the modulator bias control and to ease the modulator bias drift problem. At the output of the DP-DPMZM, two orthogonally polarized sidebands are generated with one being the RF or IF signal modulation sideband at $f_c + f_{RF}$ or $f_c - f_{IF}$, and the other being the LO modulation sideband at $f_c + f_{LO}$, where f_c, f_{RF}, f_{IF} and f_{LO} are the carrier, RF signal, IF signal and LO frequency, respectively. The two sidebands that are orthogonally polarized pass through a $LiNbO_3$ electro-optic phase modulator. By applying a DC voltage to the phase modulator, two different optical phase shifts are introduced to the two sidebands. A polarizer with its principal axis aligned with an angle of 45° relative to the

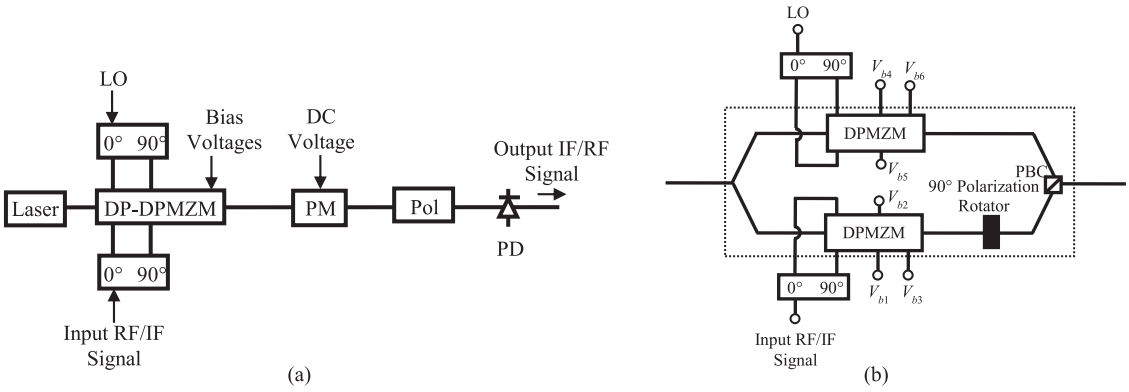

Fig. 1. (a) Schematic diagram of the dual-function photonic microwave signal processor for frequency up/down conversion and phase shifting. (b) Structure of the integrated DP-DPMZM. PM: phase modulator, Pol: polarizer, PD: photodetector, PBC: polarization beam combiner.

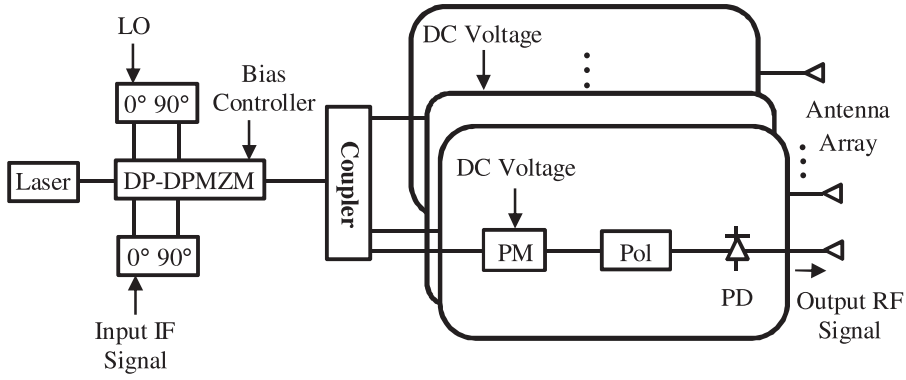

Fig. 2. Dual-function photonic microwave signal processor for use in a phased array antenna system operating in transmit mode. PM: phase modulator, Pol: polarizer, PD: photodetector.

principle axis of the phase modulator is used to make the two orthogonally polarized optical signals to have the same polarization state before detecting by a photodetector (PD). The two signals will beat at the photodetector, which generates electrical signals with the frequencies be the sum and difference between the RF/IF signal and LO frequencies.

In the case of frequency down conversion, a high-frequency input RF signal at f_{RF} is down converted to a low-frequency IF signal ($f_{IF} = f_{RF} - f_{LO}$). Similarly, a low-frequency input IF signal at f_{IF} is up converted into a high-frequency RF signal ($f_{RF} = f_{IF} + f_{LO}$) for frequency up conversion. The phase of the output IF/RF signal is determined by the optical phase difference between the RF/IF signal and LO modulation sidebands, which can be controlled by a DC voltage into the $LiNbO_3$ electro-optic phase modulator. Note that the output IF/RF signal phase shifting operation is performed in a $LiNbO_3$ electro-optic phase modulator, which is separated from input signal modulation. This is suitable for a phased array antenna system operating in the transmit mode in which each antenna element is connected to a phase modulator to control phase of the signal in each channel, and to ultimately control the direction of the radiation pattern. Fig. 2 shows the dual-function photonic microwave signal processor used for up converting a low-frequency IF signal into a high-frequency RF signal, which is transmitted via an antenna array where the beam direction is steered by controlling the phase differences of the multi-channel RF signals radiated from the antenna elements.

In the signal processor shown in Fig. 1, the single sideband suppressed carrier (SSB-SC) modulation is implemented using a DPMZM with the assistant of a 90° hybrid coupler. Since no optical filter is used to filter out one sideband, the signal processor is not sensitive to the change in the laser wavelength, which enables the signal processor to operate over a wide input RF signal frequency range when it is used for frequency down conversion. More importantly, the processor can also be used for frequency up conversion in which the DPMZM driven by a low-frequency IF signal can produce an IF signal modulation sideband, which is very close to the optical carrier. The operating frequency and bandwidth of the dual-function photonic microwave signal processor are determined by the 90° hybrid coupler bandwidth. 90° hybrid couplers with a wide bandwidth of e.g., 4−40 GHz are commercially available from manufacturers such as Marki Microwave. This enables the signal processor to be used in an electronic warfare system covering a frequency range from 4 to 40 GHz [14]. Suppressing the optical carrier in a frequency conversion system would improve the conversion efficiency as well as the isolation between the output and input port, as compared with a conventional system based on two cascaded modulators for photonic microwave mixing [15].

3. Analysis

In the dual-function photonic microwave signal processor shown in Fig. 1, each DPMZM inside the DP-DPMZM is biased to suppress the optical carrier and one sideband.

When the system is used for frequency down conversion, the bottom and top DPMZM are driven by a high-frequency RF signal and a high-frequency LO, respectively. The electric field at the output of the DP-DPMZM can be expressed as

$$E_{out,DPDPMZM} = \frac{\sqrt{2}}{2} E_{in} \sqrt{t_{ff}} \left[\left(J_1(\beta_{RF}) \cos\left(\omega_c + \omega_{RF}\right) t - J_3(\beta_{RF}) \cos\left(\omega_c - 3\omega_{RF}\right) t \right) \hat{y} \right.$$
$$\left. + \left(J_1(\beta_{LO}) \cos\left(\omega_c + \omega_{LO}\right) t - J_3(\beta_{LO}) \cos\left(\omega_c - 3\omega_{LO}\right) t \right) \hat{x} \right] \quad (1)$$

where E_{in} is the amplitude of the electric field at the input of the DP-DPMZM, t_{ff} is the insertion loss of each DPMZM and is assumed to be identical for the two DPMZMs, $J_m(x)$ is the Bessel function of the first kind of mth order, $\beta_{RF} = \pi V_{RF}/V_\pi$, V_{RF} is the input RF signal amplitude, V_π is the modulator switching voltage, ω_C, ω_{RF} and ω_{LO} are the angular frequencies of the optical carrier, the input RF signal and the LO, respectively, $\beta_{LO} = \pi V_{LO}/V_\pi$, V_{LO} is the LO amplitude, and $\hat{x}$ and $\hat{y}$ represent the two orthogonal polarization states. In additional to the fundamental sideband, a DPMZM operating as a SSB-SC modulator will also generate a third order sideband [21]. The signal at the output of the DP-DPMZM passes through a $LiNbO_3$ electro-optic phase modulator, which is used to introduce an optical phase ϕ_x and ϕ_y to each of the two orthogonally polarized signals. This is followed by a 45° polarizer. The electric field at the input of the PD is given by

$$E_{out} = \frac{1}{2} E_{in} \sqrt{t_{ff}} \sqrt{L} \left[J_1(\beta_{RF}) \cos\left(\left(\omega_c + \omega_{RF}\right) t + \phi_y\right) - J_3(\beta_{RF}) \cos\left(\left(\omega_c - 3\omega_{RF}\right) t + \phi_y\right) \right.$$
$$\left. + J_1(\beta_{LO}) \cos\left(\left(\omega_c + \omega_{LO}\right) t + \phi_x\right) - J_3(\beta_{LO}) \cos\left(\left(\omega_c - 3\omega_{LO}\right) t + \phi_x\right) \right] \quad (2)$$

where L is the total insertion loss of the phase modulator and the 45° polarizer. The photocurrent at the IF signal frequency $\omega_{IF} = \omega_{RF} - \omega_{LO}$ can be obtained from (2) and is given by

$$I_{IF} = \Re \frac{1}{4} P_{in} t_{ff} L \left[J_1(\beta_{RF}) J_1(\beta_{LO}) \right] \left[\cos\left(\left(\omega_{RF} - \omega_{LO}\right) t + \left(\phi_y - \phi_x\right)\right) \right] \quad (3)$$

where $\Re$ is the PD responsivity and P_{in} is the laser power into the DP-DPMZM. Equation (3) shows the phase of the output IF signal is the optical phase difference $\phi_y - \phi_x$ between the two orthogonally polarized sidebands. Typical modulation efficiency for a light travelling in TM polarization state inside a $LiNbO_3$ electro-optic phase modulator is four times the modulation efficiency for a light travelling in TE polarization state. Hence the relationship between the optical phase difference and the DC

voltage V_{DC} into the phase modulator can be written as

$$\phi_y - \phi_x = \frac{-3\pi V_{DC}}{4V_{\pi,PM}} \tag{4}$$

where $V_{\pi,\mathrm{PM}}$ is the switching voltage of the phase modulator for a light travelling in the TM polarization state. It can be seen from (3) and (4) that the output IF signal phase shift is linearly proportional to the DC voltage into the phase modulator. The electrical power of the output IF signal can be obtained from (3) and is given by

$$P_{IF,out} = \frac{1}{32}\Re^2 P_{in}^2 t_{ff}^{\ 2} L^2 J_1(\beta_{RF})^2 J_1(\beta_{LO})^2 R_o \tag{5}$$

where R_o is the PD load resistance. Note that the beating of the fundamental and the third order RF signal and LO modulation sidebands at the PD will also generate other frequency components. However, since these frequency components are all located at high frequencies outside the PD bandwidth except the frequency component at $3\omega_{LO} - 3\omega_{RF}$, they will not contribute to the output. The electrical power of the unwanted frequency component at $3\omega_{LO} - 3\omega_{RF}$ is given by

$$P_{3\omega_{LO}-3\omega_{RF},out} = \frac{1}{32}\Re^2 P_{in}^2 t_{ff}^{\ 2} L^2 J_3(\beta_{RF})^2 J_3(\beta_{LO})^2 R_o \tag{6}$$

Assume the input RF signal is a small signal, the ratio of the unwanted frequency component power to the output IF signal power is

$$\frac{P_{3\omega_{LO}-3\omega_{RF},out}}{P_{IF,out}} = \frac{J_3(\beta_{RF})^2 J_3(\beta_{LO})^2}{J_1(\beta_{RF})^2 J_1(\beta_{LO})^2} \approx \frac{\beta_{RF}^4 J_3(\beta_{LO})^2}{576 J_1(\beta_{LO})^2} \tag{7}$$

Equation (7) shows the unwanted frequency component at $3\omega_{LO} - 3\omega_{RF}$ is much smaller than the output IF signal and hence it has little effect on the system performance. The down conversion efficiency, which is defined as the ratio of the output IF signal power to the input RF signal power, is given by

$$G = \frac{P_{IF,out}}{P_{RF,in}} = \frac{1}{64}\Re^2 P_{in}^2 t_{ff}^{\ 2} L^2 \left(\frac{\pi}{V_\pi}\right)^2 R_{in} R_o J_1(\beta_{LO})^2 \tag{8}$$

where R_{in} is the RF port input resistance of the DP-DPMZM. Equation (8) indicates that conversion efficiency is dependent on the LO modulation index and will increase as the laser source power increases.

When the system is used for frequency up conversion, the bottom DPMZM is driven by a low-frequency IF signal and the main MZM in the bottom DPMZM is biased at a quadrature point with an opposite slope compared to that used for frequency down conversion. This would generate a lower IF signal modulation sideband, which is required to obtain an up converted RF signal at $\omega_{RF} = \omega_{IF} + \omega_{LO}$ after photodetection. The electric field at the output of the DP-DPMZM can be expressed as

$$\begin{aligned} E_{out,DPDPMZM} = \frac{\sqrt{2}}{2} E_{in}\sqrt{t_{ff}}\,[&(-J_1(\beta_{IF})\cos(\omega_c - \omega_{IF})\,t + J_3(\beta_{IF})\cos(\omega_c + 3\omega_{IF})\,t)\,\hat{y} \\ &+ (J_1(\beta_{LO})\cos(\omega_c + \omega_{LO})\,t - J_3(\beta_{LO})\cos(\omega_c - 3\omega_{LO})\,t)\,\hat{x}] \end{aligned} \tag{9}$$

where $\beta_{IF} = \pi V_{IF}/V_\pi$ and V_{IF} is the input IF signal amplitude. By following the same procedure as for frequency down conversion, the photocurrent at the RF signal frequency $\omega_{RF} = \omega_{IF} + \omega_{LO}$ and the up conversion efficiency, which is defined as the ratio of the output RF signal power to the input

IF signal power, are, respectively, given by

$$I_{RF} = -\Re\frac{1}{4}P_{in}t_{ff}L\,[J_1(\beta_{IF})J_1(\beta_{LO})]\left[\cos\left((\omega_{IF}+\omega_{LO})\,t+(\phi_x-\phi_y)\right)\right] \tag{10}$$

$$G = \frac{P_{RF,out}}{P_{IF,in}} = \frac{1}{64}\Re^2P_{in}^2{t_{ff}}^2L^2\left(\frac{\pi}{V_\pi}\right)^2R_{in}R_oJ_1(\beta_{LO})^2 \tag{11}$$

Comparing (10) and (11) with (3) and (8), we can see the signal processor operating in the up conversion mode has the same performance as operating in the down conversion mode in terms of output photocurrent and conversion efficiency. Note that, in the case of frequency up conversion, the system will also generate an unwanted frequency component at $\omega_{LO}-3\omega_{IF}$, which is close to the output RF signal. However, it has a very small output power as the unwanted frequency component at $3\omega_{LO}-3\omega_{RF}$ presented in the signal processor output when operating in the down conversion mode.

The conversion efficiency for frequency up/down conversion can be written in term of the average optical power into the PD and is given by

$$G = \frac{1}{16}\Re^2P_{avg}^2\left(\frac{\pi}{V_\pi}\right)^2R_{in}R_o\frac{1}{J_1(\beta_{LO})^2} \tag{12}$$

where P_{avg} is the average optical power into the PD, which is dominated by the LO modulation sideband amplitude, and can be expressed as

$$P_{avg} \approx \frac{1}{4}P_{in}t_{ff}L\,J_1(\beta_{LO})^2 \tag{13}$$

It can be seen from (12) that the conversion efficiency can be increased by increasing the average output optical power. It is limited by the PD optical power handling ability. Note that in practice an optical amplifier is required to ensure high average optical power into the PD to obtain a high conversion efficiency performance. However, an optical amplifier introduces signal-spontaneous beat noise, which dominates other noise components in the system. The noise figure of the dual-function photonic microwave signal processor with the inclusion of an optical amplifier is given by

$$NF = \frac{64\,(G_{OA}-1)\,n_{sp}hv}{KTP_{in}t_{ff}L\left(\frac{\pi}{V_\pi}\right)^2R_{in}R_oG_{OA}} \tag{14}$$

where G_{OA} is the optical amplifier gain, n_{sp} is the spontaneous emission factor, hv is the photon energy, K is Boltzmann constant, and T is the absolute temperature.

The above analysis indicates that two controls are required in the proposed signal processing structure. One is the DC voltage into the main MZM of the bottom DPMZM for switching from down to up conversion and vice versa. Another is the DC voltage into the optical phase modulator after the DP-DPMZM for realizing different RF/IF signal phase shifts. Commercial wide bandwidth optical phase modulators can be used to shift the RF/IF signal phase rapidly to achieve high-speed beam steering operation in a phased array beamforming system.

4. Experimental Results

Figure 3 illustrates the experimental setup of the dual-function photonic microwave signal processor for realizing frequency up/down conversion and phase shifting operation. A wavelength tunable laser, which generated a CW light at 1550 nm, was used as the optical source. The laser output power was 10 dBm. The LO for both down and up conversion was generated by a microwave generator, which was connected to the top DPMZM inside the DP-DPMZM. The RF/IF signal for down/up conversion was generated by another microwave generator and was applied to the bottom DPMZM. The insertion loss of the top and bottom DPMZM was found to be around 10 dB. A portion

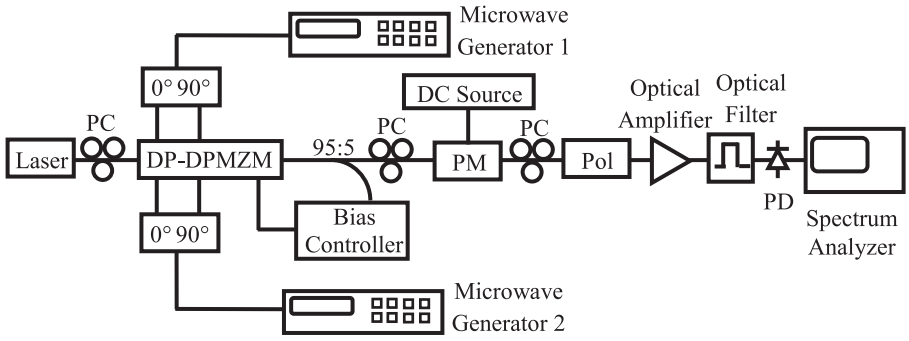

Fig. 3. Experimental setup of the dual-function photonic microwave signal processor. PC: polarization controller, PM: phase modulator, Pol: polarizer, PD: photodetector.

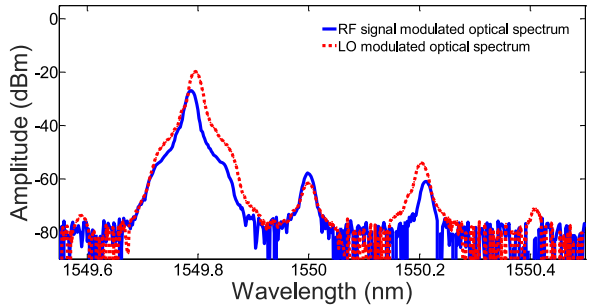

Fig. 4. Optical spectrum at the output of the phase modulator for the dual-function photonic microwave signal processor operating in the down conversion mode.

of the DP-DPMZM output was detected by a bias controller, which was used to ensure the two DPMZMs inside the DP-DPMZM were biased in the way to generate one sideband with the optical carrier being suppressed. A phase modulator, with a half-wave voltage of 4.5 V and 18 V for a light travelling in the slow and fast axis, respectively, was used to shift the output IF/RF signal phase. A polarization controller and a polarizer were used to convert the two orthogonally polarized sidebands to have the same polarization state. Since the insertion loss of the optical modulators and polarizer would degrade the signal processor conversion efficiency, a low-noise optical amplifier was used to compensate for the loss and to ensure high average optical power of 10 dBm at the input of the PD. The optical amplifier was followed by an optical filter having a 0.8 nm bandwidth and a center wavelength of 1550 nm for suppressing the amplified spontaneous emission noise. The RF/IF signal and LO sidebands were detected by a 40 GHz bandwidth PD whose output was connected to an electrical spectrum analyzer to measure the output down or up converted signal.

The down conversion ability of the signal processor was first demonstrated by driving the upper DPMZM with an LO of 25.5 GHz and the lower DPMZM with an RF signal of 26.5 GHz. Fig. 4 shows the optical spectrum measured at the output of the phase modulator. According to Fig. 4, the unwanted right sidebands and the optical carriers are well suppressed to be more than 25 dB lower than the wanted left sidebands. The optical signal-to-noise ratio, which is defined as the ratio of the first order LO modulation sideband amplitude to the highest unwanted frequency component amplitude, is 34 dB. The electrical spectrum of the down converted IF signal at 1 GHz is shown in Fig. 5. The electrical spectrums of the RF signal and LO into the signal processor are also shown in Fig. 5 for reference. The input RF signal power was -6.1 dBm and the LO power was optimized to 1.5 dBm to maximize the output IF signal power to be -7.8 dBm. A down conversion efficiency of -1.7 dB can be obtained from Fig. 5. The down converted IF signal was measured on an oscilloscope connected to the PD output for different DC voltages into the phase modulator.

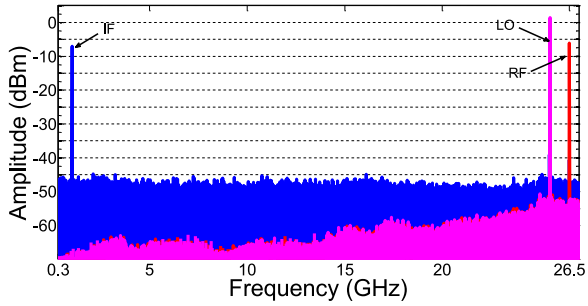

Fig. 5. Spectrums of the input RF signal and the LO. The spectrum of the frequency down-converted IF signal is also shown. The spectrum analyzer resolution bandwidth is 3 MHz.

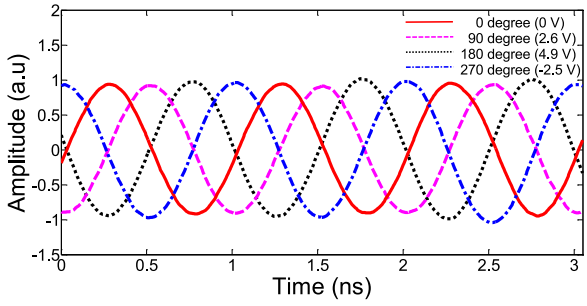

Fig. 6. Phase shifts of the down-converted IF signal with different DC voltages into the phase modulator.

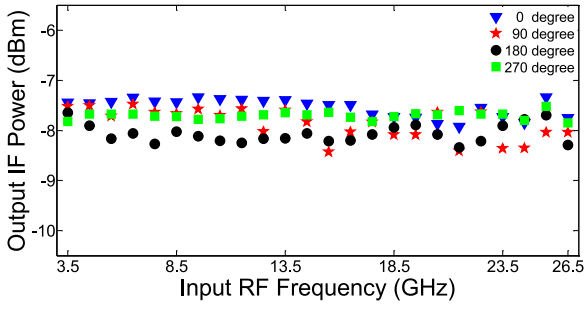

Fig. 7. IF signal power versus input RF signal frequency.

Fig. 6 shows the IF signal phase shifting operation. The experimental results demonstrate 0°–360° IF signal phase shift with almost no change in the IF signal amplitude by changing the DC voltage into the phase modulator.

The wide bandwidth capability of the dual-function photonic microwave signal processor was examined by varying the input RF signal frequency from 3.5 GHz to 26.5 GHz and adjusting the LO frequency accordingly from 2.5 to 25.5 GHz to fix the IF signal at 1 GHz. This input RF signal frequency range was limited by the 2–26.5 GHz bandwidth 90° hybrid couplers used in the experiment. Fig. 7 shows the output IF signal power for different input RF signal frequencies and different DC voltages into the phase modulator to obtain different IF signal phase shifts. There is only around 1 dB variation of the output IF signal power, which demonstrates that the signal processor is capable to operate over a wide frequency range. The down conversion efficiency was also measured when the output IF signal frequency was varied from 0.5 GHz to 3 GHz by changing the input RF signal frequency from 20.5 GHz to 23 GHz

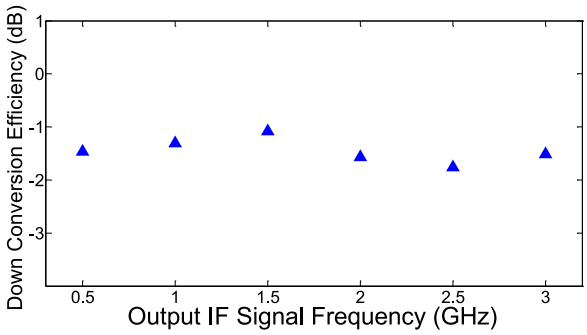

Fig. 8. Measured down conversion efficiency as a function of the IF signal frequency.

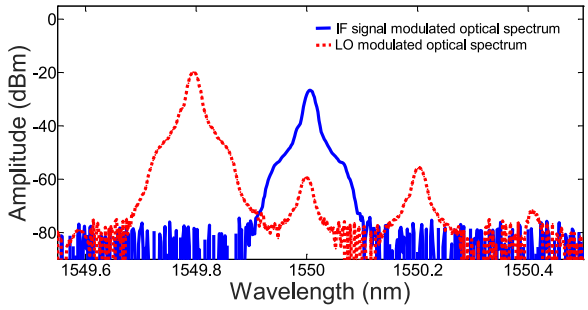

Fig. 9. Optical spectrum at the output of the phase modulator for the dual-function photonic microwave signal processor operating in the up conversion mode.

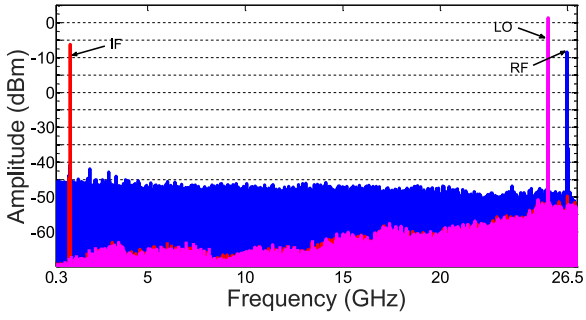

Fig. 10. Spectrums of the input IF signal and the LO. The spectrum of the frequency up-converted RF signal is also shown. The spectrum analyzer resolution bandwidth is 3 MHz.

while maintaining the LO frequency at 20 GHz. As shown in Fig. 8, the signal processor has less than 1 dB conversion efficiency variation over the 0.5 GHz to 3 GHz IF signal frequency range.

In order to demonstrate that the dual-function photonic microwave signal processor also has the ability to perform frequency up conversion, a 1 GHz IF signal with −6 dBm power was applied to the bottom DPMZM inside the DP-DPMZM via a 0.5–9 GHz bandwidth 90° hybrid coupler. The phase modulator output optical spectrum was measured and is shown in Fig. 9. Again, the residual carrier and the unwanted right sideband are more than 25 dB lower than the wanted left sideband. Fig. 10 shows the signal processor input and output electrical spectrums. It can be seen that the 1 GHz input IF signal was up converted into a 26.5 GHz RF signal at the output of the dual-function photonic microwave signal processor. The LO power required to maximize the up converted RF

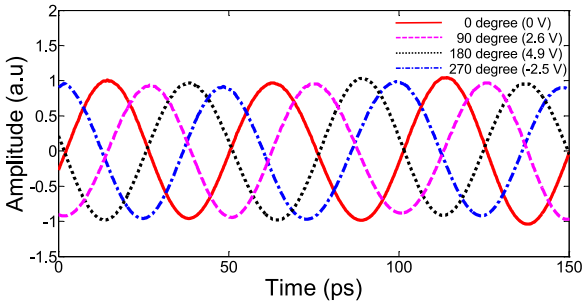

Fig. 11. Phase shifts of the up-converted RF signal with different DC voltages into the phase modulator.

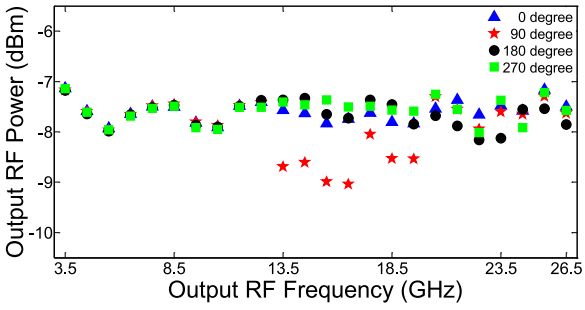

Fig. 12. RF signal power versus output RF signal frequency.

signal power is 1.5 dBm, which is the same as that used in frequency down conversion. The measurement shows that the signal processor has an up conversion efficiency of −2.2 dB. Note that around −2 dB conversion efficiency was measured for both frequency down and up conversion. This agrees with −3.4 dB conversion efficiency obtained using (12) together with the experimental parameter values such as 10 dBm output average optical power and 1.5 dBm input LO power. The experimental results also show the unwanted frequency components at the IF signal and LO frequencies are more than 32 dB below the output RF signal, which demonstrates the mixer has high isolation between the input and output port.

Figure 11 shows the output RF signals for different DC voltages into the phase modulator. The frequency of the output RF signal shown in Fig. 11 was 20 GHz, which was obtained by setting the LO frequency to 19 GHz while keeping the input IF signal frequency to be 1 GHz as before. The results demonstrate the dual-function photonic microwave signal processor operated in the up conversion mode has the ability to shift the phase of the up-converted RF signal by controlling a single modulator bias voltage. This cannot be achieved by the previously reported photonic microwave signal processors [17]. Fig. 12 shows the up-converted RF signal power for different phase shifts over the frequency range of 3.5 to 26.5 GHz, which was obtained by changing the LO frequency from 2.5 to 25.5 GHz while the IF signal frequency was fixed at 1 GHz. Fig. 13 shows the conversion efficiency when the signal processor is operating in the up conversion mode, which is around −2 dB for the input IF signal with a frequency from 0.5 to 3 GHz. This input IF signal frequency range was limited by the 2–26.5 GHz bandwidth and the 0.5–9 GHz bandwidth 90° hybrid couplers used in the experiment at the LO and IF signal port respectively. Note that the output RF signal power and the conversion efficiency measurements given in Figs. 12 and 13 have around 2 dB variation with frequency. This is due to small ripples presented in the frequency responses of the 90° hybrid couplers, DP-DPMZM and electrical cables used in the experiment.

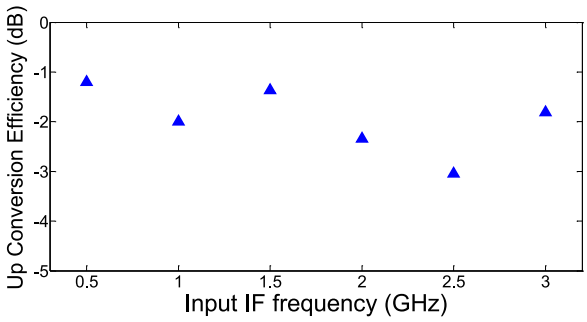

Fig. 13. Measured up conversion efficiency as a function of the input IF signal frequency.

5. Conclusion

This paper presented a novel photonic microwave signal processor that is capable to realize both frequency up/down conversion and phase shifting operation. It was implemented based on a DP-DPMZM that was biased to generate a single RF/IF signal sideband and a single LO sideband with the optical carrier being suppressed, and an optical phase modulator that was used to introduce different optical phase shifts to the two sidebands. A frequency down-converted or up-converted electrical signal with tunable phase shift was generated at the output of a photodetector. The performance of the dual-function photonic microwave signal processor was analyzed and experimentally investigated. The conversion efficiency for both frequency up and down conversion were measured to be around -2 dB and the amplitude variations of the converted signals were less than 2 dB over a wide input and output signal frequency range. A 0°–360° continuously tunable phase shift on the output IF/RF signal was demonstrated by controlling a single DC voltage into the optical phase modulator. To the best of our knowledge, this is the first time such a photonic microwave signal processor that can realize both frequency up and down conversion with high input and output isolation as well as phase shifting operation via a single control was reported.

References

[1] H. Kikuchi *et al.*, "Performance of minimum mean-square error beam forming for polarimetric phased array weather radar," *IEEE Trans. Geosci. Remote Sens.*, vol. 55, no. 5, pp. 2757–2770, May 2017.
[2] R. Y. Miyamoto and T. Itoh, "Retrodirective arrays for wireless communications," *IEEE Microw. Mag.*, vol. 3, no. 1, pp. 71–79, Mar. 2002.
[3] R. Bil and W. Holpp, "Modern phased array radar systems in Germany," in *Proc. 2016 IEEE Int. Symp. Phased Array Syst. Technol.*, 2016, pp. 1–7.
[4] W. Liu, W. Li, and J. Yao, "An ultra-wideband microwave photonic phase shifter with a full 360° phase tunable range," *IEEE Photon. Technol. Lett.*, vol. 25, no. 12, pp. 1107–1110, Jun. 2013.
[5] M. Cook and J. W. M. Rogers, "A highly compact 2.4 GHz passive 6-bit phase shifter with ambidextrous quadrant selector," *IEEE Trans. Circuits Syst. II, Exp. Briefs*, vol. 64, no. 2, pp. 131–135, Feb. 2016.
[6] Q. Zhang, C. Yuan, and L. Liu, "Studies on mechanical tunable waveguide phase shifter for phased array antenna applications," in *Proc. 2016 IEEE Int. Symp. Phased Array Syst. Technol.*, 2016, pp. 1–3.
[7] A. Natarajan, A. Komijani, X. Guan, A. Babakhani, and A. Hajimiri, "A 77-GHz phased array transceiver with on chip antennas in silicon transmitter and local LO path phase shifting," *IEEE J. Solid State Circuits*, vol. 41, no. 12, pp. 2807–2819, Dec. 2006.
[8] R. A. Minasian, E. H. W. Chan, and X. Yi, "Microwave photonic signal processing," *Opt. Exp.*, vol. 21, no. 19, pp. 22918–22936, 2013.
[9] E. H. W. Chan, W. Zhang, and R. A. Minasian, "Photonic RF phase shifter based on optical carrier and RF modulation sidebands amplitude and phase control," *J. Lightw. Technol.*, vol. 30, no. 23, pp. 3672–3678, Dec. 2012.
[10] W. Liu and J. Yao, "Ultra-wideband microwave photonic phase shifter with a 360° tunable phase shift based on an erbium-ytterbium co-doped linearly chirped FBG," *Opt. Lett.*, vol. 39, no. 4, pp. 922–924, 2014.
[11] T. Li, E. H. W. Chan, X. Wang, X. Feng, and B. Guan, "All optical photonic microwave phase shifter requiring only a single DC voltage control," *IEEE Photon. J.*, vol. 8, no. 4, Aug. 2016, Art. no. 5501008.
[12] H. Shahoei and J. Yao, "Tunable microwave photonic phase shifter based on slow and fast light effects in a tilted fiber Bragg grating," *Opt. Exp.*, vol. 20, no. 13, pp. 14009–14014, 2012.

[13] B. Wu, M. Wang, Y. Tang, J. Sun, and S. Jian, "Photonic microwave signal mixing using Sagnac loop based modulator and polarization dependent modulation," *IEEE Photon. J.*, vol. 8, no. 4, Aug. 2016, Art. no. 5501208.
[14] S. R. O'Connor, M. C. Gross, M. L. Dennis, and T. R. Clark Jr., "Experimental demonstration of RF photonic downconversion from 4-40 GHz," in *Proc. IEEE Int. Top. Meeting Microw. Photon.*, 2009, pp. 1–3.
[15] E. H. W. Chan and R. A. Minasian, "Microwave photonic downconverter with high conversion efficiency," *J. Lightw. Technol.*, vol. 30, no. 23, pp. 3580–3585, Dec. 2012.
[16] J. Zhang, E. H. W. Chan, X. Wang, X. Feng, and B. Guan, "High conversion efficiency photonic microwave mixer with image rejection capability," *IEEE Photon. J.*, vol. 8, no. 4, Aug. 2016, Art. no. 3900411.
[17] T. Jiang, S. Yu, R. Wu, D. Wang, and W. Gu, "Photonic downconversion with tunable wideband phase shift," *Opt. Lett.*, vol. 41, no. 11, pp. 2640–2643, 2016.
[18] T. Jiang, R. Wu, S. Yu, D. Wang, and W. Gu, "Microwave photonic phase-tunable mixer," *Opt. Exp.*, vol. 25, no. 4, pp. 4519–4527, 2017.
[19] H. J. Kim, J. I. Song, and H. J. Song, "An all-optical frequency up-converter utilizing four-wave mixing in a semiconductor optical amplifier for sub-carrier multiplexed radio-over-fiber applications," *Opt. Exp.*, vol. 15, no. 6, pp. 3384–3389, 2007.
[20] Y. Shi, W. Wang, and J. H. Bechtel, "High-isolation photonic microwave mixer/link for wideband signal processing and transmission," *J. Lightw. Technol.*, vol. 21, no. 5, pp. 1224–1232, May 2003.
[21] K. Higuma, S. Oikawa, Y. Hashimoto, H. Nagata, and M. Izutsu, "X-cut lithium Niobate optical single-sideband modulator," *Electron. Lett.*, vol. 37, no. 8, pp. 515–516, 2001.
[22] Fujitsu Ti:LiNbO3 DP-QPSK single-drive Mach-Zehnder modulator (FTM7977HQA) data sheet, 2014. [Online]. Available: http://www.fujitsu.com/downloads/JP/archive/imgjp/group/foc/services/100gln/ln100gdpqpsk-e-141105.pdf
[23] PlugTech Ultra compact DP-IQ modulator bias controller (MBC-DPIQ-01) data sheet, 2017. [Online]. Available: www.plugtech.hk